

## Boundary condition at a two-phase interface in the lattice Boltzmann method for the convection-diffusion equation

Hiroaki Yoshida,<sup>1,2,\*</sup> Takayuki Kobayashi,<sup>3</sup> Hidemitsu Hayashi,<sup>1</sup> Tomoyuki Kinjo,<sup>1,2</sup> Hitoshi Washizu,<sup>1,2</sup> and Kenji Fukuzawa<sup>3</sup>

<sup>1</sup>*Toyota Central R&D Labs., Inc., Nagakute, Aichi 480-1192, Japan*

<sup>2</sup>*Elements Strategy Initiative for Catalysts and Batteries (ESICB), Kyoto University, Kyoto 615-8245, Japan*

<sup>3</sup>*Graduate School of Engineering, Nagoya University, Nagoya 464-8603, Japan*

(Received 25 March 2014; published 3 July 2014)

A boundary scheme in the lattice Boltzmann method (LBM) for the convection-diffusion equation, which correctly realizes the internal boundary condition at the interface between two phases with different transport properties, is presented. The difficulty in satisfying the continuity of flux at the interface in a transient analysis, which is inherent in the conventional LBM, is overcome by modifying the collision operator and the streaming process of the LBM. An asymptotic analysis of the scheme is carried out in order to clarify the role played by the adjustable parameters involved in the scheme. As a result, the internal boundary condition is shown to be satisfied with second-order accuracy with respect to the lattice interval, if we assign appropriate values to the adjustable parameters. In addition, two specific problems are numerically analyzed, and comparison with the analytical solutions of the problems numerically validates the proposed scheme.

DOI: [10.1103/PhysRevE.90.013303](https://doi.org/10.1103/PhysRevE.90.013303)

PACS number(s): 47.11.-j, 44.05.+e, 68.05.-n

### I. INTRODUCTION

The lattice Boltzmann method (LBM), which was developed as an alternative computational scheme to conventional simulation methods such as finite-volume and finite-element methods, has recently been recognized as a powerful tool for simulating the convection and diffusion of a scalar variable [1–12]. The LBM has not only been applied to problems governed primarily by the convection-diffusion equation (CDE), such as heat transfer [13,14], reaction-diffusion system [15,16], and ion transport [17,18], but has also been used as an auxiliary to the LBM for multiphase flow simulation to handle the index variable in the phase-field method [19–21]. Boundary treatments other than the standard bounce-back rule have also been investigated in order to apply the LBM to various types of boundary conditions. For example, the partial bounce-back rule was proposed in an attempt to reproduce the heat resistance condition at the boundary [22], and special treatments to capture the curved boundaries have recently been developed [23–25]. However, the difficulty in dealing with the interface between two phases (or two media) with different transport properties remains, and most of the lattice Boltzmann algorithms are not capable of satisfying the continuity conditions of the physical variable and its flux simultaneously in a transient analysis [26,27]. Since such an interface is often encountered in many practical engineering problems, e.g., the heat-conduction problem in different materials and the ion-transport problem in porous media with different porosities, developing a scheme that satisfies the continuity conditions is very important.

In order to clarify the problem, we state the boundary conditions at the interface specifically. Let us consider a scalar

variable  $\phi$  governed by the following CDE:

$$\lambda \frac{\partial \phi}{\partial t} + \lambda \frac{\partial}{\partial x_j} (\phi v_j) = \frac{\partial}{\partial x_j} \left( K \frac{\partial \phi}{\partial x_j} \right), \quad (1)$$

where  $t$  is the time,  $K(\mathbf{x})$  is the conductivity, and  $x_j$  and  $v_j$  are the  $j$ th components of the spatial vector  $\mathbf{x}$  and the velocity of the media  $\mathbf{v}$ , respectively. The coefficient  $\lambda$  controls the relaxation speed, which corresponds to the volumetric specific heat in the heat-conduction problem. If the media is homogeneous and is characterized by a single set of  $\lambda$  and  $K$ , Eq. (1) is often divided by  $\lambda$  and the diffusivity  $D = K/\lambda$  is used as a parameter. On the other hand, if there exists an interface between two phases of different properties, the coefficient  $\lambda$  and the conductivity  $K$  appear in the boundary condition in the following form [28]:

$$\phi^A = \phi^B, \quad (2)$$

$$\left( -K^A \frac{\partial \phi^A}{\partial x_j} + v_j^A \lambda^A \phi^A \right) n_j = \left( -K^B \frac{\partial \phi^B}{\partial x_j} + v_j^B \lambda^B \phi^B \right) n_j, \quad (3)$$

where  $n_j$  is the normal unit vector on the interface, and the superscripts  $A$  and  $B$  are the indexes distinguishing the values in the different phases. Equation (2) indicates the continuity of the scalar variable, and Eq. (3) indicates the continuity of the flux. In this case, we need to specify the values of both  $\lambda$  and  $K$ . Since the relation  $D = K/\lambda$  is usually exploited in the LBM, most of the existing schemes that satisfy the conditions specified by Eqs. (2) and (3) are restricted to the analysis of steady states [13,26,27]. For the case of no background flow (or  $\mathbf{v} = 0$ ) at the interface in Eqs. (2) and (3), there are a few methods that are applicable to unsteady problems: the method proposed by Meng *et al.* for heat-conduction problems realizes the continuity of the temperature and the heat flux, assuming a plane boundary [29]. Li *et al.* have very recently proposed a method for curved interfaces, which preserves the second-order accuracy with respect to the grid interval [30].

\*h-yoshida@mosk.tytlabs.co.jp

In the present paper, we propose an alternative boundary scheme for the LBM that correctly satisfies the boundary conditions (2) and (3) at the interface between two different phases. Here a background flow  $\mathbf{v}$  across the boundary, which is important in the case of diffusion process in solvent flows through porous media, is taken into account. The present scheme is based on two simple modifications of the collision process and the streaming process, in the original LBM algorithm: (i) In each phase, a different value is assigned to the weight coefficient included in the collision term. (ii) The velocity distribution function in the LBM is multiplied (or divided) by a factor  $\gamma$  when it passes through the interface. These modifications result in new boundary conditions at the interface controlled by the ratio of the weight coefficients and the value of  $\gamma$ . Appropriate definitions of the values of these parameters enable the boundary conditions (2) and (3) to be satisfied simultaneously.

In the next section, a detailed description of the proposed algorithm is presented. The theoretical analysis in Sec. III proves that the proposed scheme reproduces the boundary conditions at the interface with second-order accuracy with respect to the lattice interval. In Sec. IV two specific problems are numerically analyzed using the present scheme. Comparison with the analytical solutions of the problems confirms that the boundary scheme appropriately approximates the boundary conditions at the interface.

## II. LATTICE BOLTZMANN METHOD

This section is dedicated to the description of the proposed algorithm. In Sec. II A we first state the lattice Boltzmann equation (LBE) used in the present study [31], and then, in Sec. II B, we describe the boundary scheme for the two-phase interface.

### A. Lattice Boltzmann equation

The LBE governs the behavior of the velocity distribution function  $f_\alpha(t, \mathbf{x})$ , which is defined for each direction labeled  $\alpha$ . (In the present paper,  $\alpha$  and  $\beta$  designate the direction of the velocity. Note that the summation convention for repeated  $\alpha$  and  $\beta$  is not assumed.) The summation of  $f_\alpha$  with respect to  $\alpha$ ,  $\phi = \sum_\alpha f_\alpha$ , approximates the solution of the CDE. Each  $f_\alpha$  travels over the uniformly distributed lattice points with the assigned velocity. In the case of three-dimensional computation, we use seven discrete velocities, which are defined in terms of  $\mathbf{e}_\alpha$ , as follows:

$$[\mathbf{e}_0, \mathbf{e}_1, \mathbf{e}_2, \mathbf{e}_3, \mathbf{e}_4, \mathbf{e}_5, \mathbf{e}_6] = \begin{bmatrix} 0 & 1 & -1 & 0 & 0 & 0 & 0 \\ 0 & 0 & 0 & 1 & -1 & 0 & 0 \\ 0 & 0 & 0 & 0 & 0 & 1 & -1 \end{bmatrix}. \quad (4)$$

The LBM for the CDE does not require the isotropy of the fourth-order tensor  $\sum_\alpha e_{\alpha i} e_{\alpha j} e_{\alpha k} e_{\alpha l}$ , in contrast to the conventional LBM for flow simulation [31]. This absence of constraint for the fourth-order tensor makes it possible to use the small number of discrete velocities as in the above equation, compared with that for the Navier-Stokes equation, in which 15 or 19 discrete velocities are usually employed.

Using the above-defined notation, the LBE is written as follows:

$$f_\alpha(t + \Delta t, \mathbf{x} + \mathbf{e}_\alpha \Delta x) - f_\alpha(t, \mathbf{x}) = \sum_\beta (\mathbf{M}^{-1} \mathbf{S} \mathbf{M})_{\alpha\beta} (f_\beta^{\text{eq}} - f_\beta)(t, \mathbf{x}), \quad (5)$$

where  $\Delta t$  is the time step, and  $\Delta x$  is the lattice interval. The equilibrium distribution function  $f_\alpha^{\text{eq}}$  is defined as follows:

$$f_\alpha^{\text{eq}}(\phi) = \left(1 + \frac{\Delta t}{2\Gamma \Delta x} v_j e_{\alpha j}\right) \omega_\alpha \phi, \quad (6)$$

$$\phi = \sum_\alpha f_\alpha, \quad (7)$$

where  $v_j$  is the  $j$ th component of the background flow velocity of the media, which is a given function. The weight coefficient  $\omega_\alpha$  is defined as

$$\omega_\alpha = \begin{cases} 1 - 6\Gamma, & (\alpha = 0) \\ \Gamma, & (\alpha = 1, \dots, 6) \end{cases}, \quad (8)$$

where  $\Gamma \in (0, 1/6)$  is a constant. The explicit form of the matrices  $\mathbf{M}$  and  $\mathbf{S}$  are

$$\mathbf{M} = \begin{pmatrix} 1 & 1 & 1 & 1 & 1 & 1 & 1 \\ 0 & 1 & -1 & 0 & 0 & 0 & 0 \\ 0 & 0 & 0 & 1 & -1 & 0 & 0 \\ 0 & 0 & 0 & 0 & 0 & 1 & -1 \\ 6 & -1 & -1 & -1 & -1 & -1 & -1 \\ 0 & 2 & 2 & -1 & -1 & -1 & -1 \\ 0 & 0 & 0 & 1 & 1 & -1 & -1 \end{pmatrix}, \quad (9)$$

$$\mathbf{S}^{-1} = \text{diag}(\tau_0, \bar{\tau}, \bar{\tau}, \bar{\tau}, \tau_4, \tau_5, \tau_6). \quad (10)$$

With the matrix  $\mathbf{M}$ , the distribution function expressed in the discrete velocity space is projected onto another vector space before the relaxation process in Eq. (5), in which the first component of  $\sum_\beta \mathbf{M}_{\alpha\beta} f_\beta$  corresponds to the conserved variable  $\phi$ , and the second to fourth components are related to the flux (or gradient) of  $\phi$ ; the rest of the components do not have significant physical meanings, but affect the computational error. The choice of the components of  $\mathbf{M}$  is discussed in Ref. [31]. The matrix  $\mathbf{S}$  controls the time required for  $f_\alpha$  to relax toward  $f_\alpha^{\text{eq}}$ . If the relaxation-time coefficient  $\bar{\tau}$  is related to  $K$  and  $\lambda$  through the equation below, the value of  $\phi$  obtained using the LBM converges to the solution of Eq. (1) in the limit of  $\Delta x \rightarrow 0$  [31]:

$$\bar{\tau} = \frac{1}{2} + \frac{\Delta t}{2\Gamma \Delta x^2} \frac{K}{\lambda}. \quad (11)$$

If the conductivity  $K$  is spatially variable,  $\bar{\tau}$  is also a function of  $\mathbf{x}$ .

Note that the multiple-relaxation-time (MRT) method is used in the collision operator as in the right-hand side of Eq. (5) supplemented with Eqs. (9) and (10). This is because the single-relaxation-time (SRT) collision operator, which is most widely used in the LBM, is not sufficiently robust to the variation of the physical relaxation time coefficient  $\bar{\tau}$ . [The present formulation reduces to the SRT collision operator while setting  $\tau_p = \bar{\tau}$  ( $p = 0, 4, 5, 6$ ).] If the SRT was used along

with the algorithm presented herein, the computational error would become very large in a certain parameter range in which  $\bar{\tau}$  becomes very large. As demonstrated in Sec. IV A, the MRT operator significantly improves the accuracy for such a severe parameter range.

The computational algorithm of the LBM consists of the two procedures based on Eq. (5). If the value of  $f_\alpha$  at time  $t$  is known, then the value at time  $t + \Delta t$  is evaluated as follows:

(i) Collision process:

$$\hat{f}_\alpha(t, \mathbf{x}) = f_\alpha(t, \mathbf{x}) + \sum_{\beta} (\mathbf{M}^{-1} \mathbf{S} \mathbf{M})_{\alpha\beta} (f_\beta^{\text{eq}} - f_\beta)(t, \mathbf{x}). \quad (12)$$

(ii) Streaming process:

$$f_\alpha(t + \Delta t, \mathbf{x} + \mathbf{e}_\alpha \Delta x) = \hat{f}_\alpha(t, \mathbf{x}). \quad (13)$$

### B. Boundary scheme at the interface

As mentioned in the introduction, in the proposed boundary scheme both the collision and streaming processes are modified. The first modification is that different values are used for the constant  $\Gamma$  in the definition of the weight coefficient, i.e.,  $\Gamma^A \neq \Gamma^B$ , with superscripts  $A$  and  $B$  denoting the values in phases A and B, respectively. Second, the streaming process (13) is replaced by the following equation:

$$f_\alpha^B(t + \Delta t, \mathbf{x} + \mathbf{e}_\alpha \Delta x) = \gamma \hat{f}_\alpha^A(t, \mathbf{x}), \quad (14)$$

$$f_{\bar{\alpha}}^A(t + \Delta t, \mathbf{x}) = (1/\gamma) \hat{f}_{\bar{\alpha}}^B(t, \mathbf{x} - \mathbf{e}_{\bar{\alpha}} \Delta x), \quad (15)$$

where  $\gamma \in (0,1)$  is a constant. The superscripts  $A$  and  $B$  are conveniently introduced to distinguish the values in the different phases, as in Eqs. (2) and (3), though the LBM in the present paper deals with a common distribution function  $f_\alpha$  throughout the computational domain. The subscript  $\bar{\alpha}$  indicates the direction opposite the direction of  $\alpha$ , i.e.,  $\mathbf{e}_\alpha = -\mathbf{e}_{\bar{\alpha}}$ . The above equation assumes that the interface is located at the halfway point between  $\mathbf{x}$  in phase A and  $\mathbf{x} + \mathbf{e}_\alpha \Delta x = \mathbf{x} - \mathbf{e}_{\bar{\alpha}} \Delta x$  in phase B. In the next section, we clarify the condition satisfied by the macroscopic quantity  $\phi$  when the protocol described herein is used and discuss how to determine the values of  $\Gamma^A$ ,  $\Gamma^B$ , and  $\gamma$  in order to satisfy the desired conditions (2) and (3).

### III. ASYMPTOTIC ANALYSIS

In this section we first outline the asymptotic analysis of the LBE [31,32], and the explicit expressions of the asymptotic solution of  $f_\alpha$ . We then analyze the boundary scheme described in Sec. II B, following the methods described in Refs. [31,33], in order to derive the relationship among the scalar variable  $\phi$  and the parameters  $\Gamma^A$ ,  $\Gamma^B$ , and  $\gamma$ .

#### A. Diffusive scaling and the asymptotic solutions

Before starting the asymptotic analysis, we rescale the time and spatial variables. We thus introduce the following rescaled variables:

$$\tilde{t} = \frac{U}{L} t, \quad \tilde{\mathbf{x}} = \frac{1}{L} \mathbf{x}, \quad \tilde{\mathbf{u}} = \frac{1}{U} \mathbf{u}, \quad (16)$$

where  $L$  and  $U$  are the reference length and speed, respectively. We choose the value of  $U$  based on the discussion in Refs. [31,32]:

$$U = C\epsilon, \quad \epsilon = \frac{\Delta x}{L}, \quad C = \frac{\Delta x}{\Delta t}. \quad (17)$$

This definition implies that the reference speed is sufficiently slower than the dynamics of the distribution function characterized by the speed  $C$ . In the asymptotic analysis,  $\epsilon$  defined in Eq. (17) is used as a small parameter; i.e., we investigate the behavior of the LBE in the limit of  $\epsilon \rightarrow 0$ .

Equation (17) defining  $U$  means that we choose the reference time as  $T = L/U = \Delta t/\epsilon^2$ . Therefore, the time variable defined in Eq. (16) is written as  $\tilde{t} = t\epsilon^2/\Delta t$ . Correspondingly, the rescaled time step  $\Delta\tilde{t} = \Delta t/T$  is  $\Delta\tilde{t} = \epsilon^2$ , which implies that the limit  $\epsilon \rightarrow 0$  must be taken while maintaining  $\Delta\tilde{t}/\epsilon^2 = 1$ .

Using the rescaled variables, the LBE is rewritten as follows:

$$f_\alpha(\tilde{t} + \epsilon^2, \tilde{\mathbf{x}} + \mathbf{e}_\alpha \epsilon) - f_\alpha(\tilde{t}, \tilde{\mathbf{x}}) = \sum_{\beta} (\mathbf{M}^{-1} \mathbf{S} \mathbf{M})_{\alpha\beta} (f_\beta^{\text{eq}} - f_\beta)(\tilde{t}, \tilde{\mathbf{x}}). \quad (18)$$

The equilibrium distribution function  $f_\alpha^{\text{eq}}$  is expressed as follows:

$$f_\alpha^{\text{eq}} = \left(1 + \epsilon \frac{\tilde{v}_j e_{\alpha j}}{2\Gamma}\right) \omega_\alpha \phi, \quad (19)$$

$$\tilde{\mathbf{v}} = \frac{1}{U} \mathbf{v}. \quad (20)$$

The scaling employed herein, which is referred to as diffusive scaling, was first developed by Sone [34] in order to prove the convergence of the continuum Boltzmann equation to the fluid-dynamic equations [35,36] and has since been widely applied to the analysis of the LBE [31,32,37,38].

The asymptotic analysis then begins by expanding  $f_\alpha$  in terms of powers of  $\epsilon$ :

$$f_\alpha = f_\alpha^{(0)} + f_\alpha^{(1)}\epsilon + f_\alpha^{(2)}\epsilon^2 + \dots. \quad (21)$$

Similarly,  $f_\alpha^{\text{eq}}$  and  $\phi$  are expanded:

$$f_\alpha^{\text{eq}} = f_\alpha^{\text{eq}(0)} + f_\alpha^{\text{eq}(1)}\epsilon + f_\alpha^{\text{eq}(2)}\epsilon^2 + \dots, \quad (22)$$

$$\phi = \phi^{(0)} + \phi^{(1)}\epsilon + \phi^{(2)}\epsilon^2 + \dots. \quad (23)$$

After substituting Eqs. (22) and (23) into Eq. (19), equating the coefficients of the same power of  $\epsilon$  yields the expression of  $f_\alpha^{\text{eq}(m)}$  in terms of  $\phi^{(m)}$ :

$$f_\alpha^{\text{eq}(0)} = \omega_\alpha \phi^{(0)}, \quad (24)$$

$$f_\alpha^{\text{eq}(1)} = \omega_\alpha \phi^{(1)} + \frac{\tilde{v}_j e_{\alpha j}}{2\Gamma} \omega_\alpha \phi^{(0)}, \quad (25)$$

$$f_\alpha^{\text{eq}(2)} = \omega_\alpha \phi^{(2)} + \frac{\tilde{v}_j e_{\alpha j}}{2\Gamma} \omega_\alpha \phi^{(1)}, \quad (26)$$

...

Next, we substitute the expansion (21) into Eq. (18), and apply the Taylor expansion to  $f_\alpha(\tilde{t} + \epsilon^2, \tilde{\mathbf{x}} + \mathbf{e}_\alpha\epsilon)$  about  $(\tilde{t}, \tilde{\mathbf{x}})$ . A series of equations for  $f_\alpha^{(m)}$  is then obtained by equating the coefficients of the same power of  $\epsilon$ . These equations are solved from the lowest power using Eqs. (24) through (26). Here we summarize the results necessary in the analysis of the boundary scheme, the details of which are described in Ref. [31]:

$$f_\alpha^{(0)} = \omega_\alpha \phi^{(0)}, \quad (27)$$

$$f_\alpha^{(1)} = \omega_\alpha \phi^{(1)} + \frac{\tilde{v}_j e_{\alpha j}}{2\Gamma} \omega_\alpha \phi^{(0)} - \sum_\beta (\mathbf{M}^{-1} \mathbf{S}^{-1} \mathbf{M})_{\alpha\beta} e_{\beta j} \frac{\partial f_\beta^{(0)}}{\partial \tilde{x}_j}, \quad (28)$$

$$f_\alpha^{(2)} = \omega_\alpha \phi^{(2)} + \frac{\tilde{v}_j e_{\alpha j}}{2\Gamma} \omega_\alpha \phi^{(1)} - \sum_\beta (\mathbf{M}^{-1} \mathbf{S}^{-1} \mathbf{M})_{\alpha\beta} \times \left( \frac{\partial f_\beta^{(0)}}{\partial \tilde{t}} + e_{\beta j} \frac{\partial f_\beta^{(1)}}{\partial \tilde{x}_j} + \frac{e_{\beta j} e_{\beta k}}{2} \frac{\partial^2 f_\beta^{(0)}}{\partial \tilde{x}_j \partial \tilde{x}_k} \right). \quad (29)$$

In the process of obtaining the above results, it is found that the inhomogeneous terms in the linear equations for  $f_\alpha^{(m)}$  ( $m \geq 2$ ) must satisfy the solvability conditions. In particular, the solvability conditions of the equations for  $f_\alpha^{(2)}$  and  $f_\alpha^{(3)}$  are effectively the same as the CDE (1) for  $\phi^{(0)}$  and  $\phi^{(1)}$ , respectively. We then prove that the numerical solution of the LBM appropriately approximates the solution of the CDE (1).

## B. Analysis of the boundary scheme

We now analyze the boundary scheme described in Sec. II B, by means of a similar expansion method [31,33]. In the course of the analysis, the explicit forms of the asymptotic solutions (24) through (29) are used to transform the conditions for the distribution function into those for the scalar variable  $\phi$ . Here we restrict ourselves to the case in which the interface passes through the midpoint between the two lattice points, at which the expansion is conducted:  $\tilde{\mathbf{x}}_C = \tilde{\mathbf{x}} + \mathbf{e}_\alpha\epsilon/2 = \tilde{\mathbf{x}} - \mathbf{e}_{\bar{\alpha}}\epsilon/2$  ( $\mathbf{e}_{\bar{\alpha}} = -\mathbf{e}_\alpha$ ). Equations (14) and (15) are rewritten in terms of  $\tilde{\mathbf{x}}_C$  as follows:

$$f_\alpha^B(\tilde{t} + \epsilon^2, \tilde{\mathbf{x}}_C + \mathbf{e}_\alpha\epsilon/2) = \gamma \left[ f_\alpha^A(\tilde{t}, \tilde{\mathbf{x}}_C - \mathbf{e}_\alpha\epsilon/2) + \sum_\beta (\mathbf{M}^{-1} \mathbf{S} \mathbf{M})_{\alpha\beta} (f_\beta^{\text{eq}A} - f_\beta^A)(\tilde{t}, \tilde{\mathbf{x}}_C - \mathbf{e}_\alpha\epsilon/2) \right], \quad (30)$$

$$f_{\bar{\alpha}}^A(\tilde{t} + \epsilon^2, \tilde{\mathbf{x}}_C + \mathbf{e}_{\bar{\alpha}}\epsilon/2) = \frac{1}{\gamma} \left[ f_{\bar{\alpha}}^B(\tilde{t}, \tilde{\mathbf{x}}_C - \mathbf{e}_{\bar{\alpha}}\epsilon/2) + \sum_\beta (\mathbf{M}^{-1} \mathbf{S} \mathbf{M})_{\bar{\alpha}\beta} (f_\beta^{\text{eq}B} - f_\beta^B)(\tilde{t}, \tilde{\mathbf{x}}_C - \mathbf{e}_{\bar{\alpha}}\epsilon/2) \right]. \quad (31)$$

In a manner similar to that described in Sec. III A, we substitute the expansion of Eqs. (21) and (22) into the above equations and apply the Taylor expansion about  $(\tilde{t}, \tilde{\mathbf{x}}_C)$ . Then, the conditions at the interface that should be satisfied by  $f_\alpha^{(m)}$  are obtained by equating the coefficients of the same power of  $\epsilon$ . With the aid of the asymptotic solutions, these conditions are expressed in terms of  $\phi^{(m)}$ .

In the leading order ( $\epsilon^0$ ), the following condition is obtained from Eq. (30):

$$f_\alpha^{B(0)} = \gamma \left[ f_\alpha^{A(0)} + \sum_\beta (\mathbf{M}^{-1} \mathbf{S} \mathbf{M})_{\alpha\beta} (f_\beta^{\text{eq}A(0)} - f_\beta^{A(0)}) \right], \quad (32)$$

where the argument  $(\tilde{t}, \tilde{\mathbf{x}}_C)$  is omitted for the sake of simplicity. Substituting Eqs. (24) and (27) yields the following condition for  $\phi^{(0)}$ :

$$\gamma \Gamma^A \phi^{A(0)} = \Gamma^B \phi^{B(0)}. \quad (33)$$

Here  $\omega_\alpha = \Gamma$  ( $\alpha \neq 0$ ) has been used [Eq. (8)]. In addition to Eq. (32), a similar relation is obtained from Eq. (31), which ends up with the same condition for  $\phi^{(0)}$  as Eq. (33).

Proceeding to the next order ( $\epsilon$ ), we obtain the following conditions:

$$\frac{e_{\alpha j}}{2} \frac{\partial f_\alpha^{B(0)}}{\partial \tilde{x}_j} + f_\alpha^{B(1)} = \gamma \left\{ -\frac{e_{\alpha j}}{2} \frac{\partial f_\alpha^{A(0)}}{\partial \tilde{x}_j} + f_\alpha^{A(1)} + \sum_\beta (\mathbf{M}^{-1} \mathbf{S} \mathbf{M})_{\alpha\beta} \left[ -\frac{e_{\alpha j}}{2} \frac{\partial}{\partial \tilde{x}_j} (f_\beta^{\text{eq}A(0)} - f_\beta^{A(0)}) + (f_\beta^{\text{eq}A(1)} - f_\beta^{A(1)}) \right] \right\}, \quad (34)$$

$$\frac{e_{\bar{\alpha} j}}{2} \frac{\partial f_{\bar{\alpha}}^{A(0)}}{\partial \tilde{x}_j} + f_{\bar{\alpha}}^{A(1)} = \frac{1}{\gamma} \left\{ -\frac{e_{\bar{\alpha} j}}{2} \frac{\partial f_{\bar{\alpha}}^{B(0)}}{\partial \tilde{x}_j} + f_{\bar{\alpha}}^{B(1)} + \sum_\beta (\mathbf{M}^{-1} \mathbf{S} \mathbf{M})_{\bar{\alpha}\beta} \left[ -\frac{e_{\bar{\alpha} j}}{2} \frac{\partial}{\partial \tilde{x}_j} (f_\beta^{\text{eq}B(0)} - f_\beta^{B(0)}) + (f_\beta^{\text{eq}B(1)} - f_\beta^{B(1)}) \right] \right\}. \quad (35)$$

We then substitute the asymptotic solutions (24), (25), (27), and (28), to obtain the following conditions for  $\phi^{(0)}$  and  $\phi^{(1)}$ :

$$\gamma \Gamma^A \phi^{A(1)} = \Gamma^B \phi^{B(1)}, \quad (36)$$

$$\gamma \left( -\tilde{D}^A \frac{\partial \phi^{A(0)}}{\partial \tilde{x}_j} + \tilde{v}_j^A \phi^{A(0)} \right) e_{\alpha j} = \left( -\tilde{D}^B \frac{\partial \phi^{B(0)}}{\partial \tilde{x}_j} + \tilde{v}_j^B \phi^{B(0)} \right) e_{\alpha j}, \quad (37)$$

where  $\tilde{D} = 2\Gamma(\bar{\tau} - 1/2)$ . If we proceed to the analysis of the second order ( $\epsilon^2$ ), we similarly obtain the conditions for  $\phi^{(1)}$  and  $\phi^{(2)}$ . Here we write only the condition for  $\phi^{(1)}$ :

$$\begin{aligned} & \gamma \left( -\tilde{D}^A \frac{\partial \phi^{A(1)}}{\partial \tilde{x}_j} + \tilde{v}_j^A \phi^{A(1)} \right) e_{\alpha j} \\ & = \left( -\tilde{D}^B \frac{\partial \phi^{B(1)}}{\partial \tilde{x}_j} + \tilde{v}_j^B \phi^{B(1)} \right) e_{\alpha j}. \end{aligned} \quad (38)$$

Next, we integrate the conditions (33), (36), (37), and (38) by using  $\phi = \phi^{(0)} + \phi^{(1)}\epsilon + \dots$ , and rewrite them in terms of the variables before rescaling. Then  $\phi$  is found to satisfy the following conditions at the interface with second-order accuracy with respect to the lattice interval:

$$\gamma \Gamma^A \phi^A = \Gamma^B \phi^B, \quad (39)$$

$$\gamma \left( -\frac{K^A}{\lambda^A} \frac{\partial \phi^A}{\partial x_j} + v_j^A \phi^A \right) n_j = \left( -\frac{K^B}{\lambda^B} \frac{\partial \phi^B}{\partial x_j} + v_j^B \phi^B \right) n_j. \quad (40)$$

Relation (11) was used in obtaining Eq. (40). Clearly, the desired boundary conditions (2) and (3) are satisfied if the following relation among  $\gamma$ ,  $\Gamma^A$ , and  $\Gamma^B$  holds:

$$\gamma = \frac{\Gamma^B}{\Gamma^A} = \frac{\lambda^A}{\lambda^B}. \quad (41)$$

The values of  $\Gamma^A$  and  $\Gamma^B$  are not unique in the range  $(0, 1/6)$ , because only the ratio is specified in Eq. (41). In the numerical analysis in Sec. IV, we assign the value of  $1/8$  to the larger  $\Gamma$ . Note that the choice of the value of  $\Gamma$  affects the relaxation-time coefficient  $\bar{\tau}$  through Eq. (11). Therefore the value of the time step  $\Delta t$  should be carefully chosen, in the case of an extreme value for  $\Gamma$ , because the value of  $\bar{\tau}$  influences the numerical errors, as will be discussed in Sec. IV A.

#### IV. NUMERICAL ANALYSIS

In this section we numerically examine the boundary scheme described in Sec. II B with the parameter setting (41), in order to confirm that it correctly satisfies the boundary conditions at a two-phase interface. For this purpose, we consider in Sec. IV A the convection-diffusion process near a plane interface between two phases, and in Sec. IV B the diffusion in a core-shell sphere with an interface between the core and the shell. In both problems, the numerical results are compared to the exact solutions.

##### A. Convection and diffusion near a plane interface

We consider two phases (or media) that are streaming in the  $x$  direction, while keeping the interface at  $x = 0$ . Phases A and B are in the regions  $x > 0$  and  $x < 0$ , respectively, and the values of  $\lambda$  and  $K$  are constant but different in the two regions ( $\lambda^A \neq \lambda^B$ ,  $K^A \neq K^B$ ). The velocities of phase A and B are  $v_x^A$  and  $v_x^B$ , respectively. We investigate the diffusion process of a scalar variable  $\phi$  using Eq. (1). A physical example of this problem is ion diffusion in an electrolyte solution flowing through two porous media with different porosities  $\lambda^A$  and  $\lambda^B$  in contact. Then the scalar variable  $\phi$  is identified with the ion

concentration, with  $K$  being the effective diffusion coefficient in the porous media. Note that, in this case, the relation  $\lambda^A v_x^A = \lambda^B v_x^B$  should hold because of mass conservation for the electrolyte solution.

Initially,  $\phi = \phi^{\text{in}}$  in  $x > 0$ , and  $\phi = 0$  in  $x < 0$ , and the boundary conditions at  $x = 0$  are given in the following form:

$$\phi^A = \phi^B, \quad (42)$$

$$-K^A \frac{\partial \phi^A}{\partial x} + v_x^A \lambda^A \phi^A = -K^B \frac{\partial \phi^B}{\partial x} + v_x^B \lambda^B \phi^B. \quad (43)$$

This initial- and boundary-value problem in the case of  $v_x^A = v_x^B = 0$  (pure diffusion case) has the following exact solution [39]:

$$\phi^A(t, x) = \frac{\phi^{\text{in}}}{1 + \Lambda} \left[ 1 + \text{Lerf} \left( \frac{x}{2\sqrt{K^A t / \lambda^A}} \right) \right], \quad (44)$$

$$\phi^B(t, x) = \frac{\phi^{\text{in}}}{1 + \Lambda} \text{erfc} \left( -\frac{x}{2\sqrt{K^B t / \lambda^B}} \right), \quad (45)$$

where  $\Lambda = (\lambda^B K^B / \lambda^A K^A)^{1/2}$ . On the other hand, the exact solution in the case of  $v_x^A \neq 0$  and  $v_x^B \neq 0$  is obtained via Laplace transformation as follows:

$$\phi^m(t, x) = -\frac{1}{\pi} \int_0^\infty 2\text{Im}[\Phi^m(w^2 e^{i\pi}, x)] e^{-w^2 t} w dw, \quad (46)$$

$$\Phi^A(s, x) = \frac{1}{s} [F(s) - \phi^{\text{in}}] \exp \left[ \frac{x v_x^A}{2D^A} - \frac{x G^A(s)}{2} \right] + \frac{\phi^{\text{in}}}{s}, \quad (47)$$

$$\Phi^B(s, x) = \frac{1}{s} F(s) \exp \left[ \frac{x v_x^B}{2D^B} + \frac{x G^B(s)}{2} \right], \quad (48)$$

$$F(s) = \frac{\phi^{\text{in}} [K^A G^A(s) - v_x^A \lambda^A]}{\lambda^A v_x^A - \lambda^B v_x^B + K^A G^A(s) + K^B G^B(s)}, \quad (49)$$

$$G^m(s) = \left[ \left( \frac{v_x^m}{D^m} \right)^2 + \frac{4s}{D^m} \right]^{1/2}, \quad (50)$$

where superscript  $m$  indicates the phase ( $m = A, B$ ), and  $i$  is the imaginary unit. (Recall  $D^m = K^m / \lambda^m$ .) In Eq. (46),  $\text{Im}[\cdot]$  denotes the imaginary part of the argument. Since  $\text{Im}[\Phi^m]$  decays as  $w \rightarrow \infty$ , the numerical values of the exact solution are obtained with integrating Eq. (46) over a finite range.

Whereas the exact solution is for the infinite domain  $x \in (-\infty, \infty)$ , the LBM computation is carried out in a bounded domain  $x \in (-20L, 20L)$  with  $L$  being a reference length. The periodic condition is assumed in the  $y$  and  $z$  directions, restricting the domain to  $y, z \in (0, L)$ . The lattice interval is  $\Delta x = L/N$ , and the time step is  $(K^A / \lambda^A L^2) \Delta t = 0.125 \times (1/N)^2$ . The present problem is characterized by the four dimensionless parameters:  $\lambda^B / \lambda^A$ ,  $K^B / K^A$ ,  $(\lambda^A L / K^A) v_x^A$ , and  $(\lambda^B L / K^A) v_x^B$ .

Figure 1 shows the time evolution of the profile of  $\phi$  for the case of  $\lambda^B / \lambda^A = 0.5$  and  $K^B / K^A = 0.5^{3/2}$ . The lattice interval is  $\Delta x = L/40$ . The diffusion layer, in which a steep gradient of  $\phi$  is observed, is formed adjacent to the interface

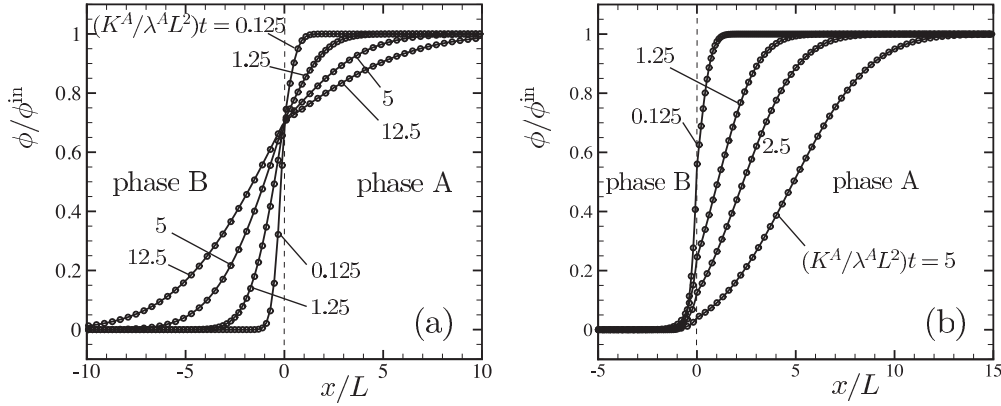


FIG. 1. Time evolution of the profiles of  $\phi$  around the interface for the case of  $\lambda^B/\lambda^A = 0.5$  and  $K^B/K^A = 0.5^{3/2}$ . (a)  $v_x^A = v_x^B = 0$  and (b)  $(\lambda^A L/K^A)v_x^A = (\lambda^B L/K^A)v_x^B = 1$ . The symbol indicates the LBM results, and the solid line indicates the exact solutions given in Eqs. (44) and (45) [panel (a)], and Eq. (46) [panel (b)].

in the short-time regime and then relaxes and becomes thicker as time advances. In the case of  $v_x^A = v_x^B = 0$ , as indicated by both the exact solution [Eqs. (44) and (45)] and Fig. 1(a), the value of  $\phi$  at the interface is constant independent of time. On the other hand, in the case of  $(\lambda^A L/K^A)v_x^A = (\lambda^B L/K^A)v_x^B = 1$  [Fig. 1(b)], the diffusion layer flows in the  $x$  direction and the value of  $\phi$  at the interface decreases as time advances. The LBM results are in agreement with the exact solution, including the discontinuity of the gradient at the interface [Eq. (43)], which shows that the boundary scheme described in Sec. II B with the parameter set given in Eq. (41) works correctly.

In the theoretical analysis described in Sec. III, the accuracy of the scheme is predicted to be of the second order with respect to the lattice interval (or  $\epsilon$ ). In order to examine the theoretical prediction, we show, in Fig. 2, the errors defined by  $E_\infty = \max |\phi^{\text{numerical}} - \phi^{\text{exact}}|/\phi^{\text{in}}$  and  $E_2 = [\sum_x (\phi^{\text{numerical}} - \phi^{\text{exact}})^2/N_E]^{1/2}/\phi^{\text{in}}$  as functions of the lattice interval  $\Delta x$ . The sum in the definition of  $E_2$  runs over the lattice points in  $-5L \leq x \leq 5L$ , and then  $N_E = 10N$ . The errors are estimated at time  $(K^A/\lambda^A L^2)t = 1.25$ . Since the log-log plots of the errors are parallel to the line having a slope equal to 2, the scheme is shown to possess second-order accuracy.

The magnitude of the error also depends on the value of  $\lambda^B/\lambda^A$  (and  $K^B/K^A$ ). This is because the relaxation-time coefficients are dependent on  $\lambda$  and  $K$  through Eq. (11), and the error then depends on the relaxation-time coefficient. In order to suppress the increase in the error for small values of  $\lambda^B/\lambda^A$ , in the present paper, we used the multiple-relaxation-time (MRT) method in the collision operator as defined in Eq. (5) with Eqs. (9) and (10). We demonstrate the improvement in accuracy achieved by using the MRT method. Figure 3 compares the errors for various values of  $\lambda^B/\lambda^A$  with those obtained using the ordinary single-relaxation-time (SRT) method. More specifically, in the SRT computation, we set  $\tau_p = \bar{\tau}$  ( $p = 0, 4, 5, 6$ ), whereas in the MRT computation,  $\tau_p$  ( $p = 0, 4, 5, 6$ ) is maintained at unity irrespective of the value of  $\bar{\tau}$ . The collision operator of the SRT method, which is often referred to as the BGK operator, is the most widely used operator because of its simplicity. One of the drawbacks of this operator, however, is that the error is very sensitive to the variation of the relaxation-time coefficient, which is crucial in the application of the present boundary scheme, as shown in Fig. 3. This is the reason we use a rather complicated MRT in the present paper.

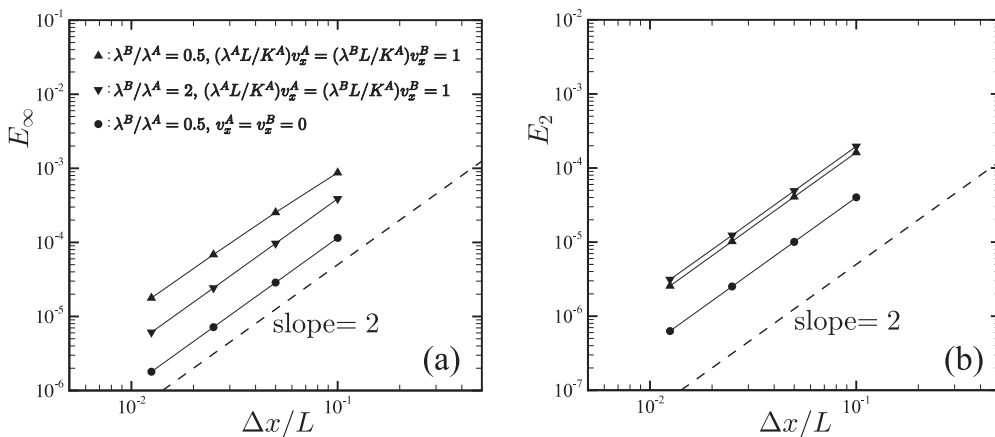


FIG. 2. Error versus the lattice interval in the plane-interface problem. (a)  $E_\infty$  and (b)  $E_2$ . The value of conductivity ratio is  $K^B/K^A = (\lambda^B/\lambda^A)^{3/2}$ . A dashed line indicating a slope of 2 is also shown in the figure.

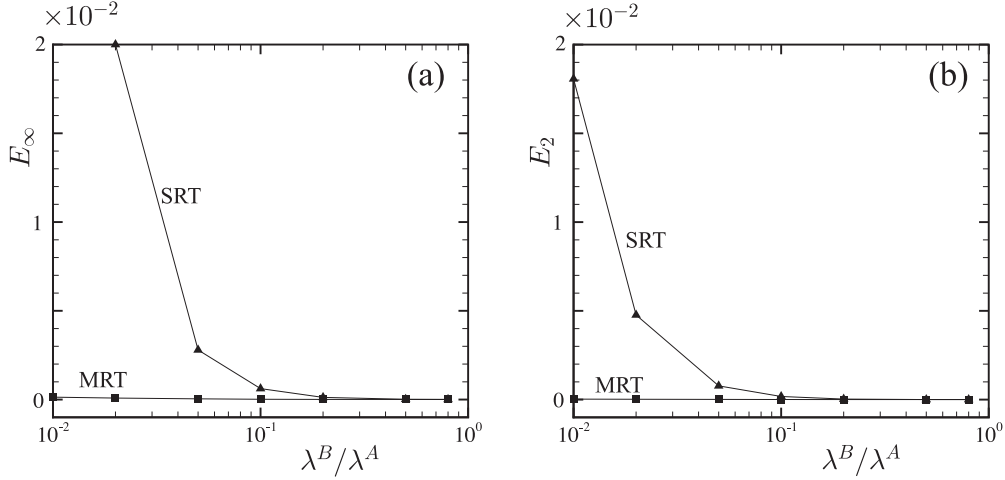


FIG. 3. Error versus  $\lambda^B/\lambda^A$  in the plane-interface problem for the case of  $v_x^A = v_x^B = 0$  and  $K^B/K^A = (\lambda^B/\lambda^A)^{3/2}$ . (a)  $E_\infty$  and (b)  $E_2$ . The lattice interval is fixed at  $\Delta x/L = 0.025$ . The symbol  $\blacksquare$  indicates the results obtained using the multiple-relaxation-time (MRT) collision operator, and the symbol  $\blacktriangle$  indicates the results obtained using the single-relaxation-time (SRT) collision operator.

The conductivity  $K$  in Eq. (1) is in general spatially variable. Here we check the continuity of  $\phi$  and its flux at the interface for such a case using a similar one-dimensional problem. To this end, we replace the constant  $K$  by  $K(1 + a\sqrt{|x/L|})$  in the above problem, with  $a$  being a constant parameter. Table I lists the values of  $\phi$  and the flux  $J = -K(\partial\phi/\partial x) + v\lambda\phi$  at the interface, with the superscripts  $A$  and  $B$  indicating the values at  $x = 0+$  and  $x = 0-$ , respectively. Clearly, the continuity of  $\phi$  and  $J$  realized using the present scheme is not violated by the spatial variation of  $K$ . In the numerical tests here, the lattice interval is  $\Delta x = L/20$ , and other parameters are the same as those of the case in Fig. 1(b). Since the interface is located at the midpoint between two lattice points, the values in the table are measured by means of the second-order polynomial extrapolation, using the values of  $\phi$  at the lattice points around the interface at the instant  $(K^A/\lambda^A L^2)t = 1.25$ .

### B. Diffusion in a core-shell sphere

Let us consider a sphere with a core filled with another phase (or media). The core shares its center with the shell at  $x = 0$ , and the radii of the core and the shell are  $R^A$  and  $R^B$ , respectively (Fig. 4). We investigate the behavior of the scalar variable  $\phi$  inside the sphere, based on the diffusion equation. The values of  $(\lambda, K)$  are constant and denoted by  $(\lambda^A, K^A)$  in  $0 < r < R^A$ , and  $(\lambda^B, K^B)$  in  $R^A < r < R^B$ , with  $r$  being the radial coordinate, i.e.,  $r = (x^2 + y^2 + z^2)^{1/2}$ . Initially the value of  $\phi$  is uniform in the sphere, i.e.,  $\phi = \phi^{\text{in}}$  at  $t = 0$  in  $0 < r < R^B$ . The surface of the sphere ( $r = R^B$ ) is maintained at  $\phi = 0$  for  $t > 0$ . The internal boundary condition at  $r = R^A$  is

described by Eqs. (2) and (3) without the background velocity  $\mathbf{v}$ . This initial- and boundary-value problem has the following exact solution [40]:

$$\phi^A(t, r) = \frac{2R^B\phi^{\text{in}}}{r} \sum_{n=1}^{\infty} \frac{1}{g(\theta_n)} \sin(r\theta_n) \sin(R^A\theta_n) \times \sin[(R^B - R^A)k\theta_n] \exp[-(K^A/\lambda^A)\theta_n^2 t], \quad (51)$$

$$\phi^B(t, r) = \frac{2R^B\phi^{\text{in}}}{r} \sum_{n=1}^{\infty} \frac{1}{g(\theta_n)} \sin^2(R^A\theta_n) \times \sin[(R^B - r)k\theta_n] \exp[-(K^A/\lambda^A)\theta_n^2 t], \quad (52)$$

where

$$g(\theta_n) = \frac{R^A\theta_n}{\Lambda} \sin^2[(R^B - R^A)k\theta_n] + (R^B - R^A)k\theta_n \sin^2(R^A\theta_n) + \frac{1 - k/\Lambda}{R^A k\theta_n} \sin^2[(R^B - R^A)k\theta_n] \sin^2(R^A\theta_n), \quad (53)$$

$$k = \left(\frac{\lambda^B K^A}{\lambda^A K^B}\right)^{1/2}, \quad \Lambda = \left(\frac{\lambda^B K^B}{\lambda^A K^A}\right)^{1/2}, \quad (54)$$

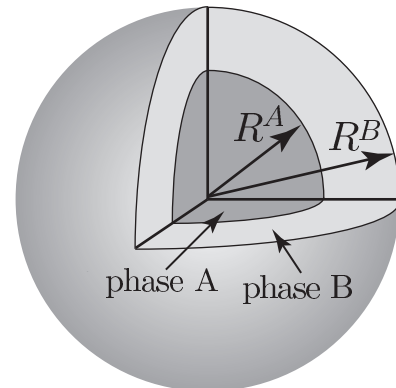


FIG. 4. Core-shell sphere with two phases.

TABLE I. Continuity check for the case of spatially variable  $K$ .

$a$	$\phi^A/\phi^{\text{in}}$	$\phi^B/\phi^{\text{in}}$	$(L/\phi^{\text{in}}K^A)J^A$	$(L/\phi^{\text{in}}K^A)J^B$
1	0.5989	0.5988	0.5565	0.5565
10	0.6833	0.6833	0.6688	0.6688
100	0.7555	0.7556	0.7410	0.7411

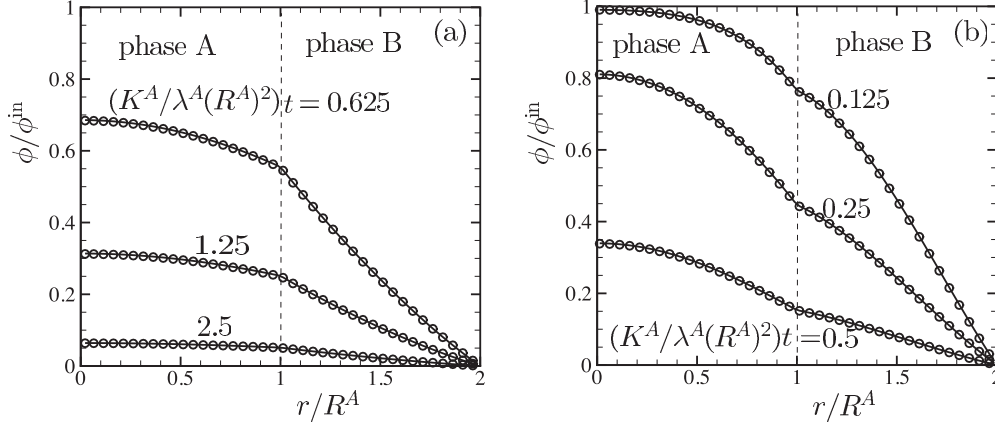


FIG. 5. Time evolution of the profiles of  $\phi$  in the radial direction in the core-shell sphere. (a)  $\lambda^B/\lambda^A = 0.5$  and  $K^B/K^A = 0.5^{3/2}$  and (b)  $\lambda^B/\lambda^A = 2$  and  $K^B/K^A = 2^{3/2}$ . The symbol indicates the LBM results, and the solid line indicates the exact solution given in Eqs. (51) and (52).

and  $\theta_i$  is the root of the following equation for  $\theta$ :

$$K^B \{ R^A k \theta \cot[(R^B - R^A)k\theta] + 1 \} + K^A [R^A \theta \cot(R^A \theta) - 1] = 0. \quad (55)$$

Note that the above solution is valid only for the irrational values of  $k(R^B - R^A)/R^A$ ; otherwise correction terms are necessary [40]. In the present paper, we consider only the cases in which  $k(R^B - R^A)/R^A$  is irrational.

Although the problem is one-dimensional in the radial direction, in order to examine the capability of handling a curved interface, we carry out the three-dimensional LBM computation using a Cartesian coordinate system, in which the lattice points in  $0 < r \leq R^A$  belong to phase A and the points in  $R^A < r < R^B$  belong to phase B. The computational domain is restricted to  $x, y, z \in (0, R^B)$ , imposing the symmetric boundary condition (no-gradient condition) at the planes  $x = 0$ ,  $y = 0$ , and  $z = 0$ . The other parameters, such as the lattice interval and the time step, are specified similarly to those in Sec. IV A, choosing  $R^A$  as the reference length. In Fig. 5 we show the time evolution of the profiles of  $\phi$  in the case of  $R^B/R^A = 2$ . The lattice interval is  $\Delta x = R^A/40$ . In the case of  $\lambda_B/\lambda_A = 0.5$  and  $K^B/K^A = 0.5^{3/2}$  [Fig. 5(a)], since the conductivity is higher in phase A, the gradient of  $\phi$  relaxes and the profile flattens faster than that in phase B. On the other hand, in the case of  $\lambda_B/\lambda_A = 2$  and  $K^B/K^A = 2^{3/2}$  [Fig. 5(b)], the gradient of  $\phi$  remains in phase A because of the lower conductivity. In both cases, the LBM results correctly capture the behavior of the exact solution, which demonstrates the applicability of the proposed scheme to the case of a curved boundary. Note that in Fig. 5, the value of  $\phi$  at  $r$  is obtained by averaging the values at all of the lattice points within the gap  $r - \Delta x/2 < (x^2 + y^2 + z^2)^{1/2} \leq r + \Delta x/2$ .

Finally, we investigate the accuracy in greater detail. In Fig. 6 we show the error  $E_\infty$  (defined in Sec. IV A) as a function of the lattice interval. Since, in the three-dimensional LBM, the spherical interface at  $r = R^A$  and the surface at  $r = R^B$  are approximated by the stepwise voxel data, the convergence of the positions of the interface and the boundary exhibits first-order accuracy with respect to the lattice interval. This is why the error of the results obtained using the Cartesian

coordinates exhibits first-order accuracy. In the figure, for comparison, we also show the results of the one-dimensional LBM in the spherical polar coordinate system (see Ref. [41] for details of the LBM in curvilinear coordinate systems). The second-order accuracy observed in the case of the spherical polar coordinates, in which the interface and boundary pass through the halfway point between two lattice points, also confirms that the deceleration of the convergence in the Cartesian coordinates is due to the approximation accuracy of the position of the interface and the boundary. The absolute values of the error are sensitive to the value of  $\lambda^B/\lambda^A$  in the case of the spherical polar coordinates. This is because the benefit of using the multiple-relaxation-time collision operator is less pronounced if we use the one-dimensional LBM in which the relaxation-time matrix is small [41]. Another point observed in Fig. 6 is that, in the range of the lattice interval

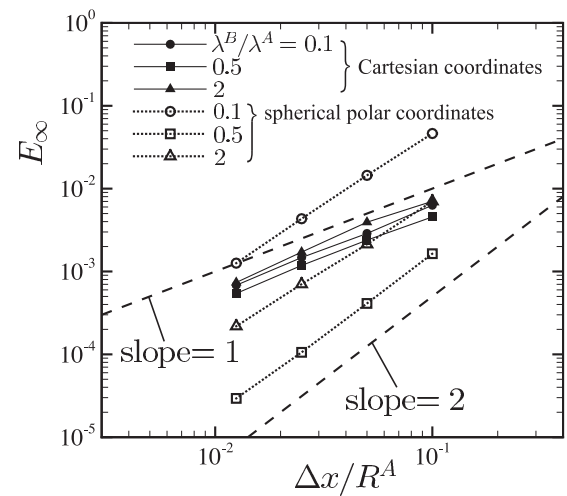


FIG. 6. Error versus the lattice interval in the core-shell sphere problem for the cases of  $\lambda^B/\lambda^A = 0.1, 0.5, \text{ and } 2$ ;  $K^B/K^A = (\lambda^B/\lambda^A)^{3/2}$ . The filled symbols indicate the results of the three-dimensional LBM using Cartesian coordinates, and the open symbols indicate the results of the one-dimensional LBM using spherical polar coordinates. Dashed lines indicating slopes of 1 and 2 are also shown.

size investigated herein, the errors of the two results are comparable, which implies that the simple algorithm of the proposed scheme is promising for practical applications, in which curved boundaries exist. If the second-order accuracy is essential in analyzing a problem with curved boundaries using a Cartesian grid, the method proposed recently by Li *et al.* [30] is a promising alternative. Note that, however, if a background velocity across the boundary exists, one must extend the method in Ref. [30], though the extension should be straightforward.

## V. SUMMARY

We have proposed a modified algorithm of the lattice Boltzmann method (LBM) at the two-phase interface, which includes new parameters, i.e., the ratio of the weight coefficients in the equilibrium distribution function and the factor that multiplies (or divides) the distribution function in the streaming process. The asymptotic analysis of the algorithm, which is based on the method in Refs. [31,33], shows that the boundary conditions described in Eqs. (39) and (40) are satisfied with second-order accuracy with respect to the lattice interval, if the interface passes through the median point between lattice points. The new boundary conditions (39) and (40) are correctly reduced to the desired boundary conditions, i.e., Eqs. (2) and (3), by applying the relation (41) among the parameters appearing in the scheme.

We numerically analyzed two specific problems, i.e., an expanding diffusion layer adjacent to a plane interface, and

the relaxation process in a sphere with a core. The results for the former problem numerically confirmed the theoretically predicted second-order accuracy. In addition, the necessity of the multiple-relaxation-time collision operator was also demonstrated. In the latter problem, although the convergence was decelerated, the leading-order accuracy was guaranteed even if we approximate the shape of the interface by means of the voxel data, and the applicability of the scheme to the curved interface was confirmed.

One possible extension of the present research is to incorporate a jump of the scalar variable at the interface, an example of which is the interfacial thermal resistance in heat-conduction problems. If the jump at the interface is prescribed as a ratio, the present scheme is directly applied with tuning the values of  $\Gamma$  and  $\gamma$  in Eq. (39). However, the prescribed difference of the scalar variable, e.g., the Kapitza resistance of the form  $(\phi^A - \phi^B)/(\partial\phi/\partial x) = \text{const}$ , is not covered by the present scheme. In that case, combining the present scheme and the partial bounce-back scheme [22,38], which realizes a jump condition prescribed as a difference, would be a promising approach.

## ACKNOWLEDGMENTS

The authors thank S. Iwai for computer assistance. The present work was partially supported by MEXT program “Elements Strategy Initiative to Form Core Research Center” (since 2012). (MEXT stands for Ministry of Education, Culture, Sports, Science and Technology, Japan.)

- 
- [1] E. G. Flekkøy, *Phys. Rev. E* **47**, 4247 (1993).
  - [2] S. P. Dawson, S. Chen, and G. D. Doolen, *J. Chem. Phys.* **98**, 1514 (1993).
  - [3] H. W. Stockman, R. J. Glass, C. Cooper, and H. Rajaram, *Int. J. Mod. Phys. C* **09**, 1545 (1998).
  - [4] R. M. H. Merks, A. G. Hoekstra, and P. M. A. Sloot, *J. Comput. Phys.* **183**, 563 (2002).
  - [5] I. Ginzburg, *Adv. Water Resour.* **28**, 1171 (2005).
  - [6] M. Stiebler, J. Tölke, and M. Krafczyk, *Comput. Math. Appl.* **55**, 1576 (2008).
  - [7] B. C. Shi, B. Deng, R. Du, and X. W. Chen, *Comput. Math. Appl.* **55**, 1568 (2008).
  - [8] B. C. Shi and Z. Guo, *Phys. Rev. E* **79**, 016701 (2009).
  - [9] S. G. Ayodele, F. Varnik, and D. Raabe, *Phys. Rev. E* **80**, 016304 (2009).
  - [10] I. Ginzburg, *Commun. Comput. Phys.* **11**, 1439 (2012).
  - [11] J. Wang, D. Wang, P. Lallemand, and L.-S. Luo, *Comput. Math. Appl.* **65**, 262 (2013).
  - [12] Z. Chai and T. S. Zhao, *Phys. Rev. E* **87**, 063309 (2013).
  - [13] M. Wang, J. Wang, N. Pan, and S. Chen, *Phys. Rev. E* **75**, 036702 (2007).
  - [14] L. Li, R. Mei, and J. F. Klausner, *Int. J. Heat Mass Transf.* **67**, 338 (2013).
  - [15] R. Blaak and P. M. A. Sloot, *Comput. Phys. Commun.* **129**, 256 (2000).
  - [16] S. G. Ayodele, F. Varnik, and D. Raabe, *Phys. Rev. E* **83**, 016702 (2011).
  - [17] X. He and N. Li, *Comput. Phys. Commun.* **129**, 158 (2000).
  - [18] Y. Akinaga, S. Hyodo, and T. Ikeshoji, *Phys. Chem. Chem. Phys.* **10**, 5678 (2008).
  - [19] T. Inamura, T. Ogata, S. Tajima, and N. Konishi, *J. Comput. Phys.* **198**, 628 (2004).
  - [20] A. Fakhari and M. H. Rahimian, *Phys. Rev. E* **81**, 036707 (2010).
  - [21] N. Takada, J. Matsumoto, and S. Matsumoto, *J. Comput. Sci. Tech.* **7**, 322 (2013).
  - [22] K. Han, Y. T. Feng, and D. R. J. Owen, *Int. J. Therm. Sci.* **47**, 1276 (2008).
  - [23] I. Ginzburg, *Adv. Water Resour.* **28**, 1196 (2005).
  - [24] T. Gebäck and A. Heintz, *Commun. Comput. Phys.* **15**, 487 (2014).
  - [25] L. Li, R. Mei, and J. F. Klausner, *J. Comput. Phys.* **237**, 366 (2013).
  - [26] J. Wang, M. Wang, and Z. Li, *Int. J. Therm. Sci.* **46**, 228 (2007).
  - [27] A. Tarokh, A. A. Mohamad, and L. Jiang, *Numer. Heat Transf. Part A* **63**, 159 (2013).
  - [28] X. Chen and P. Han, *Int. J. Heat Fluid Flow* **21**, 463 (2000).
  - [29] F. Meng, M. Wang, and Z. Li, *Int. J. Heat Fluid Flow* **29**, 1203 (2008).
  - [30] L. Li, C. Chen, R. Mei, and J. F. Klausner, *Phys. Rev. E* **89**, 043308 (2014).
  - [31] H. Yoshida and M. Nagaoka, *J. Comput. Phys.* **229**, 7774 (2010).
  - [32] M. Junk, A. Klar, and L.-S. Luo, *J. Comput. Phys.* **210**, 676 (2005).

- [33] M. Junk and Z. Yang, *J. Stat. Phys.* **121**, 3 (2005).
- [34] Y. Sone, in *Advances in Kinetic Theory and Continuum Mechanics*, edited by R. Gatignol and J. B. Soubbaramayer (Springer, Berlin, 1991), pp. 19–31.
- [35] Y. Sone, K. Aoki, S. Takata, H. Sugimoto, and A. V. Bobylev, *Phys. Fluids* **8**, 628 (1996).
- [36] Y. Sone, *Kinetic Theory and Fluid Dynamics* (Birkhäuser, Boston, 2002).
- [37] T. Inamuro, M. Yoshino, and F. Ogino, *Phys. Fluids* **9**, 3535 (1997).
- [38] H. Yoshida and H. Hayashi, *J. Stat. Phys.* **155**, 277 (2014).
- [39] J. Crank, *The Mathematics of Diffusion*, 2nd ed. (Oxford University Press, New York, 1975).
- [40] H. S. Carslaw and J. C. Jaeger, *Conduction of Heat in Solids*, 2nd ed. (Oxford University Press, New York, 1986).
- [41] H. Yoshida and M. Nagaoka, *J. Comput. Phys.* **257**, 884 (2014).